CIRCUIT THEORY AND APPLICATIONS, VOL. 3, 339–354 (1975)

A NEW APPROACH TO THE NETWORK MODELLING OF CAPACITIVE IRISES AND STEPS IN WAVEGUIDE

T. E. ROZZI

Philips Research Laboratories, Eindhoven, The Netherlands

SUMMARY

Classical network representations of waveguide discontinuities assume monomode operation and involve elements which depend not only upon geometry, but also on frequency.

Later approaches to the problem consist of numerical techniques. These are unsuitable for synthesis since they do not yield equivalent networks and involve repeating the field analysis at each frequency, which is cumbersome for applications to wideband design.

A recent approach permits to derive wideband equivalent networks with elements which depend only upon geometry. In this contribution capacitive irises, steps and combinations are treated. These discontinuities occur in filters, transformers, etc. where higher-order mode interaction cannot be neglected for closely spaced discontinuities. Whatever this spacing may be, higher order mode interaction always occurs in oversize guide. Higher order mode interaction fits naturally into the network modelling presented here. The resulting network representations are either in canonical Foster form of the first type or easily reducible to it. This approach is based on a Rayleigh–Ritz variational solution of the field problem and involves manipulations with small matrices only.

The accuracy of the method is demonstrated for a number of basic configurations, while its flexibility is illustrated by providing simpler equivalent networks, applicable when extreme accuracy is not required. The elements involved are given in graphical or in simple analytical form.

1. INTRODUCTION

Accurate wideband network models of discontinuities in standard and oversize waveguide, are important for the optimum design of modern microwave telecommunication systems. Approximate narrow-band monomode representations of single capacitive irises and steps are familiar to the microwave engineer.[1] First order variational and quasi-static solutions are treated in References 2 and 3. The relative convergence phenomenon arising in the application of the moments method to the iris problem is discussed in Reference 4. An analytical solution is known for the infinitely thin capacitive semidiaphragm in standard guide (Reference 2, p. 452), while the interaction between two closely spaced identical infinitely thin irises has also been investigated.[5]

However neither a true wideband equivalent circuit for one mode nor any equivalent circuit at all for more than one mode is available. The latter is required when treating either the interaction between closely spaced discontinuities in standard waveguide or discontinuities in oversize guide. The principles of a new approach to the modelling of transverse aperture type discontinuities in a general multimode situation has been presented in recent contributions.[6,7] This approach is based upon the following physical considerations:

(i) Only the first higher order modes excited by a discontinuity 'see' the successive discontinuity, that is, all the propagating modes plus possibly the first few non-propagating ones. All these we shall call accessible modes.

(ii) All other modes, infinite in number, can be considered as localized to the neighbourhood of the discontinuity which excites them. Also, their propagation constants approach their quasi-static limits for increasing order.

Received 7 February 1975
Revised 21 April 1975

Accessible modes represent the truly distributed part of the problem. Localized modes instead, being almost 'lumped' in nature, are responsible for the energy storage of the discontinuity. The total effect of the localized modes on the accessible ones can be represented by lossless, reciprocal, quasi-lumped multiports (one pair of accessible ports for each accessible mode). These multiports admit a Foster canonical representation. The problem consists in extracting poles and residues directly from the Rayleigh–Ritz variational solution of the field problem. Here an important role is played by the lumped approximation of the modal characteristic admittances appearing in the Green's function.

Once the network representation of a single discontinuity, having possibly more than one accessible mode, has been determined, the problem of a cascade of interacting discontinuities reduces to the network analysis of a cascade of lumped multiports connected by a finite (and usually small) number of transmission lines (see Figure 1). The elements of the multiports are known, and so are the propagation constants of the transmission lines.

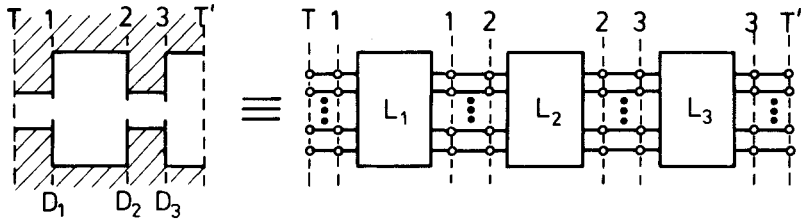

Figure 1. Cascade of interacting irises

Inductive irises and steps under arbitrary TE(LSM) excitation have been treated in a recent paper.[8] Here the characteristic admittances of the localized modes are modelled by means of antiresonant LC circuits, in such a way as to allow the extraction of the canonical form of the reactance from its 'spot-frequency' variational expression.

The same technique is also applicable to the treatment of obstacle problems under TM excitation. However, in the dual case of TM (LSE) excitation of aperture-type discontinuities or TE (LSM) excitation of obstacle-type discontinuities, the technique of Reference 8 is less suitable, due to the form of the frequency dependence of the Green's function.

The present contribution treats the above problem specialized to the case of the capacitive iris and step discontinuity. More general discontinuities, exciting TE as well as TM modes simultaneously, can be treated by combining the techniques of Reference 8 and the one given here.

In this paper a number of examples are discussed, namely, the infinitely thin semidiaphragm, the E-plane step, the thick iris, two closely spaced interacting irises. Network models are provided for these cases. The element values are given in graphical or in simple analytic form as functions of the geometry, so that the designer not interested in the theoretical derivation, can refer directly to this information, without having to work the examples out and refer to a computer program.

2. FIELD PROBLEM OF AN INFINITELY THIN IRIS AND STEP DISCONTINUITY

The step and the iris can be recovered as particular cases of the infinitely thin diaphragm at the junction of two semi-infinite guides having different height, defined in Figure 2(a).

Because of symmetry considerations, the above situation is electrically equivalent to that of a symmetric iris of aperture 2d at the junction of two waveguides having height 2b and 2b′ respectively. A TE_{10} mode incident upon the discontinuity from the left, excites higher-order LSE_{1n} modes in guide g. These can be derived from a x-directed magnetic vector potential with the only component

$$\Pi_h = \sin\frac{\pi x}{a} \cdot \varphi(y) \cdot e^{-\Gamma_{nz}} \tag{1}$$

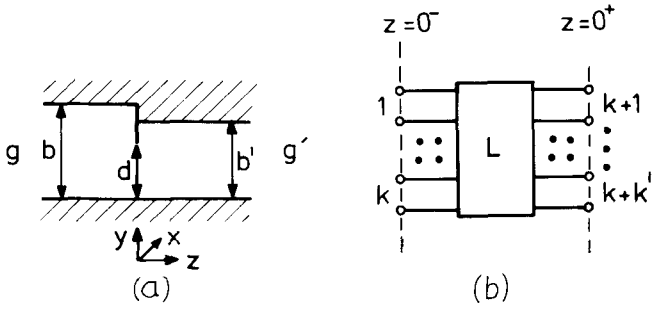

Figure 2. (a) Iris/step geometry, (b) network representation

where a is the guide width and Γ_n the propagation constant. Application of the boundary conditions at $y = 0, b$ to (1) yields the following y-dependence of the transverse modal fields in guide g:

$$\varphi_0 = \sqrt{\left(\frac{1}{2}\right)}; \qquad \varphi_n(y) = \cos\frac{n\pi y}{b}: \qquad n > 0 \tag{2a}$$

while in guide g' it becomes:

$$\psi_0 = \sqrt{\left(\frac{b}{2b'}\right)}, \qquad \psi_m(y) = \sqrt{\left(\frac{b}{b'}\right)}\cos\frac{m\pi y}{b'}: \qquad m > 0 \tag{2b}$$

The propagation constants are now given by:

$$\Gamma_n = \left[\left(\frac{n\pi}{b}\right)^2 + \left(\frac{\pi}{a}\right)^2 - \left(\frac{2\pi}{\lambda}\right)^2\right]^{\frac{1}{2}} \qquad (\Gamma_0 = j\beta = \gamma_0) \qquad \text{in guide } g$$

$$\gamma_m = \left[\left(\frac{m\pi}{b'}\right)^2 + \left(\frac{\pi}{a}\right)^2 - \left(\frac{2\pi}{\lambda}\right)^2\right]^{\frac{1}{2}} \qquad \text{in guide } g'$$

The corresponding characteristic admittances, normalized to free space, are $Y_{0n} = j\omega\varepsilon_0/\Gamma_n$, etc. Normalizing to the admittance of the fundamental mode in the larger guide merely replaces $\omega\varepsilon_0$ by β, where β is defined as $-j\Gamma_0$. We consider k accessible modes in guide g ($n = 0, \ldots, k-1$) and k' accessible modes in guide g' ($m = 0, \ldots, k'-1$). Consequently the junction is described by a lossless, reciprocal k_a-port $k+k' \equiv k_a$. Port numeration as well as positioning of the reference planes is indicated in Figure 2(b). At the location of the iris, the waveguide susceptance (imaginary part of the modified Green's function) is the parallel combination (sum) of the waveguide susceptances of the two semi-infinite guides.[6]

The sum is taken *over the localized modes* only, while the accessible modes are treated separately by means of transmission lines connected to the accessible ports. The total normalized susceptance is then:

$$\mathscr{B}(y, y') = \sum_{n \geq k} \frac{\beta}{\Gamma_n}\varphi_n(y)\varphi_n(y') + \sum_{m \geq k'} \frac{\beta}{\gamma_m}\psi_m(y)\psi_m(y') \tag{2}$$

It is convenient to transform the above into a susceptance *matrix* by means of the following change of variables[3]

$$\cos\frac{\pi y}{b} = P_{10} + P_{11}\cos\theta \equiv \alpha_1 + \alpha_2\cos\theta \tag{3}$$

with $\theta = 0$, at $y = 0, b$ and $\alpha_1 \equiv P_{10} = \cos^2(\pi d/2b)$; $\alpha_2 \equiv P_{11} = 1 - \alpha_1$; from (3), we obtain then the *finite* expansion

$$\cos\frac{n\pi y}{b} = \sum_{p=0}^{n} P_{np}\cos p\theta \tag{4}$$

(3) is formally identical to the change of variables used in the inductive iris case[8] and recursive formulas for the coefficients P_{np} can be found there. Also, ordinary Fourier analysis gives:

$$\cos\frac{m\pi y}{b'} = \sum_{p=0}^{\infty} A_{mp}\cos p\theta \tag{5}$$

where

$$A_{mp} = \frac{2}{\varepsilon_{po}\pi}\int_0^{\pi}\cos\frac{m\pi}{b'}y(\theta)\,.\cos p\theta\,.\,d\theta$$

$$A_{00} = 1;\quad \varepsilon_{po} = \varepsilon_{op}\begin{cases}2 \text{ if } p = 0\\ 1 \text{ if } p > 0\end{cases} \tag{6}$$

Owing to (4), φ_n corresponds to the n-dimensional *row* vector

$$\frac{\varepsilon_{0*}}{\sqrt{(\varepsilon_{n0})}}P_{n*} \tag{7a}$$

(A factor $\pi/2$, which does not contribute to the reactance will be suppressed consistently.)

Owing to (5), ψ_m corresponds to the infinite row vector

$$\frac{\varepsilon_{0*}}{\sqrt{(\varepsilon_{m0})}}\left(\frac{b}{b'}\right)A_{m*} \tag{7b}$$

In the following, the row vector Q_{i*} will stand for (7a) with $i = n+1$, if $i \leqslant k$ or for (7b), with $i = m+k+1$, if $i \geqslant k$.

Also, (2) corresponds to the matrix

$$\mathbf{B}_{pq} = \sum_{n\geqslant k}\frac{\beta}{\Gamma_n}P_{np}P_{nq}\varepsilon_{po}\varepsilon_{qo} + \sum_{m\geqslant k'}\frac{b}{b'}\frac{\beta}{\gamma_m}A_{mp}A_{mq}\varepsilon_{po}\varepsilon_{qo} \qquad (0 \leqslant p, q) \tag{8}$$

In the foregoing matrix representation, the $(k_a \times k_a)$-reactance matrix of the network L of Figure 2(b) is given in Reference 6

$$x_{ij} = x_{ji} = \mathbf{Q}_i\,.\,\mathbf{B}^{-1}\,.\,\mathbf{Q}_j^{\mathrm{T}}; \qquad 1 \leqslant i, j \leqslant k_a \tag{9a}$$

or

$$\mathbf{x} = \mathbf{x}^{\mathrm{T}} = \mathbf{Q}\,.\,\mathbf{B}^{-1}\,.\,\mathbf{Q}^{\mathrm{T}} \tag{9b}$$

In principle, **B** is an infinite matrix. However, a finite truncation of order N yields the Nth order Rayleigh–Ritz variational approximation of the exact value of the reactance. Since $Q_{k+1*} = \sqrt{(b/b')}Q_{1*}$ the $(k+1)$th row and column of x, corresponding to the fundamental mode of guide g', are proportional to the first row and column. Therefore we need only consider a (k_a-1)-dimensional matrix **x**.

For $k = k' = 1$, Figure 2(b) reduces to the current monomode representation consisting of a shunt reactance x and of an ideal transformer of turn ratio $\sqrt{(b/b')}$ at the junction of the two guides.

Figure 3 shows the network interpretation of (9b). The ideal transformer of (matrix) turns ratio **Q** transforms the reactance $\mathbf{B}^{-1}$ on the iris into the reactance **x** in the guide.

If $b = b'$, one recovers the case of an infinitely thin iris in waveguide. Then we have $k = k'$, and (8) reduces to

$$\mathbf{B}_{pq} = \sum_{n\geqslant k}\frac{2\beta}{\Gamma_n}P_{np}P_{nq}\varepsilon_{po}\varepsilon_{qo} \tag{10}$$

Because of symmetry, the $(2k \times 2k)$-matrix **x** can be partitioned in form identical $k \times k$-submatrices **x**′.

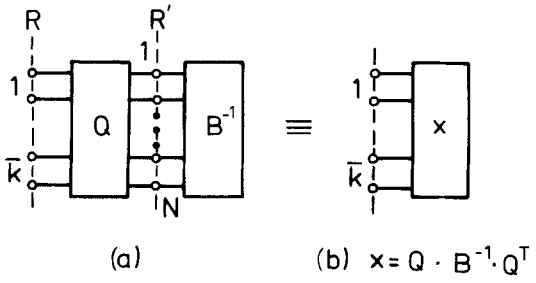

Figure 3. Block representation of (9(b))

$$\mathbf{x} = \begin{matrix} k\{ \\ k\{ \end{matrix} \overbrace{\left(\begin{array}{c|c} \mathbf{x}' & \mathbf{x}' \\ \hline \mathbf{x}' & \mathbf{x}' \end{array} \right)}^{k \quad k}; \qquad \mathbf{x} = \mathbf{x}'^{\mathrm{T}}$$

In the following $\bar{k}$ will denote either k if $b = b'$ or $k+k'-1 = k_a-1$ if $b > b'$.

3. FREQUENCY DEPENDENCE

Figure 2(b) shows the discontinuity as a linear lossless reciprocal k_a-port L, whose (normalized) reactance is given by (9) at each frequency. In fact, L must be almost lumped, due to the choice of the reference planes and to the definition of the localized modes, responsible for the energy storage represented by L.

With a view to obtaining a lumped network model for L, we observe that frequency enters (8) and (9) only *via* the propagation constants Γ_n, γ_m and β. Γ_n and γ_m are real quantities which approach their quasi-static limit for increasing order. For convenience, let us define the normalized frequency $\bar{\omega}$, $\bar{\omega} \equiv 2a/\lambda$ so that $\bar{\omega} = 1$ at cutoff

Also

$$\delta_n \equiv \frac{b}{na}; \qquad \bar{\beta}^2 \equiv \left(\frac{\pi}{a}\beta\right)^2 = \bar{\omega}^2 - 1 \tag{11}$$

The normalized characteristic susceptance of the nth mode is then

$$\beta/\Gamma_n = \delta_n \cdot \bar{\beta}/\sqrt{(1-\delta_n^2\bar{\beta}^2)} \to \delta_n\bar{\beta} \quad \text{for } n \to \infty \tag{12}$$

Let us recall the continued fraction expansion of the square root, given in Reference 9:

$$\sqrt{(1+p)^2} = 1 + \frac{\frac{1}{2}p^2}{1+\frac{1}{4}p^2/1+\ldots} \tag{13}$$

Introducing in (12) successive truncations of (13), we obtain the following positive real (pr) lumped approximations of the normalized characteristic susceptance (12), which are lumped in the 'frequency' variable $\bar{\beta}$:

$$\beta/\Gamma_n \simeq \delta_n\bar{\beta} \simeq \frac{\delta_n\bar{\beta}}{1-\frac{1}{2}\delta_n^2\bar{\beta}^2} \simeq \delta_n\bar{\beta}\frac{4-\delta_n^2\bar{\beta}^2}{4-3\delta_n^2\bar{\beta}^2} = \frac{1}{3}\bar{\beta}\,\delta_n + \frac{\frac{2}{3}\cdot\delta_n\bar{\beta}}{1-\frac{3}{4}\delta_n^2\bar{\beta}^2} \tag{14}$$

The network representations are illustrated in Figure 4. Clearly, the above are also pr lumped approximations of the unnormalized characteristic susceptance in the real frequency variable ω. As a typical example, the maximum relative error of the third order approximation in (14) over the band $1 < \bar{\omega} < 2$ in standard waveguide ($b/a = 4/9$) is equal to 1·92 per cent for $n = 1$; for $n = 2$ it reduces to 0·19 per cent.

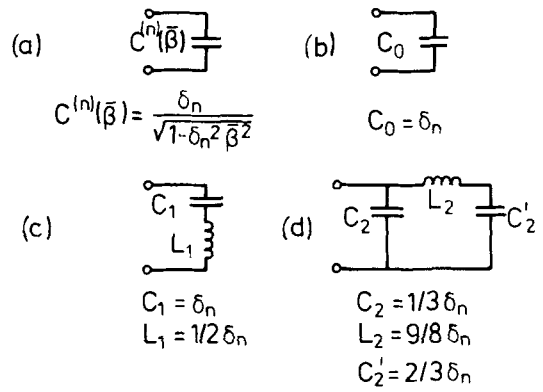

Figure 4. Lumped approximation of the characteristic admittance of LSE_{1n} modes

Let us retain the third order approximation, corresponding to the circuit of Figure 4(d), for modes of order $n \leqslant n_d$, with n_d arbitrary, and improve it, whenever necessary, by means of a further term.

The same approximation gives 'a fortiori' better result in guide g', where the normalized characteristic susceptance of the mth mode is

$$\beta/\gamma_m = \delta'_m \cdot \bar{\beta}/\sqrt{(1-\delta'^2_m\bar{\beta}^2)}; \qquad \left(\delta'_m = \frac{b'}{ma};\ b'/b \leqslant 1\right) \tag{15}$$

We replace the characteristic admittance of the remaining localized modes ($n > n_d$ in guide g and $m > m_d$ in guide g') by their quasi-static limits (i.e. the first order approximation in (14).

While introducing the above simplifications in (2), let us also rearrange the sum by adding and subtracting the quasi-static contribution of the modes in guide g with $1 \leqslant n \leqslant n_d$, so that the quasi-static sum can be put in close form, as discussed in Reference 3. The susceptance matrix **B** of (8) becomes then:

$$\mathbf{B} = \bar{\beta}\mathbf{S} + \sum_{n=k}^{n_d} \frac{\frac{2}{3}\bar{\beta}}{1-\frac{3}{4}\delta_n^2\bar{\beta}^2} D^{(n)} + \sum_{m=k'}^{m_d} \frac{\frac{2}{3}\bar{\beta}}{1-\frac{3}{4}\delta'_m\bar{\beta}^2} \mathbf{D}'^{(m)} \tag{16}$$

where

$$S_{pq} = \eta_{pq} - \sum_{n=1}^{n_d} D_{pq}^{(n)} + \sum_{m>md} D_{pq}'^{(m)} + \sum_{n=k}^{n_d} \tfrac{1}{3} D_{pq}^{(n)} + \sum_{m=k'}^{md} \tfrac{1}{3} D_{pq}'^{(m)}; \qquad (0 \leqslant p, q \leqslant N-1)$$

$$D_{pq}^{(n)} = \delta_n P_{np} P_{nq} \varepsilon_{po} \varepsilon_{qo} \tag{17a}$$

$$D_{pq}'^{(m)} = \delta_m A_{mp} A_{mq} \varepsilon_{po} \varepsilon_{qo} \tag{17b}$$

$$\eta_{pq} = \frac{b}{a} \begin{cases} 0 & : \quad \text{for } p \neq q \\ 4 \ln\left(\csc\dfrac{\pi d}{2b}\right) & : \quad \text{for } p = q = 0 \\ 1/p & : \quad \text{for } p = q > 0 \end{cases} \tag{17c, 17d}$$

B is the susceptance of the localized modes, as seen *on the iris*, i.e. the driving point susceptance of the network to the right of R' in Figure 3(a). In order to obtain the susceptance **y**, as seen by the accessible modes, i.e. as seen from R, we have to apply the inverse of the previous ideal transformer embedding.

Consider now the expression (9b) for the reactance of the accessible modes with $\bar{k} = N$. Straightforward inversion yields:

$$\mathbf{x}^{-1} = (\mathbf{Q} \cdot \mathbf{B}^{-1} \cdot \mathbf{Q}^{\mathrm{T}})^{-1} = \mathbf{U}^{\mathrm{T}} \cdot \mathbf{B} \cdot \mathbf{U} = \mathbf{y}$$
$$(\mathbf{U} \equiv \mathbf{Q}^{-1}) \tag{18}$$

In particular, if $b = b'$ or $k' = 1$ then $\mathbf{Q}$ and its inverse $\mathbf{U}$ assume lower triangular form so that any submatrix of $\mathbf{U}$ is the inverse of the corresponding submatrix of $\mathbf{Q}$. Introducing (16) in the above, we obtain a canonical Foster representation of the iris susceptance as seen by $\bar{k} = N$ accessible modes:

$$\mathbf{y}(\bar{\beta}) \approx \mathbf{C}^S\bar{\beta} + \sum_{n=K}^{n_d} \frac{\bar{\beta}\mathbf{r}^{(n)}}{1-(\bar{\beta}/\bar{\omega}_n)^2} + \sum_{m=K'}^{m_d} \frac{\bar{\beta}\mathbf{r}'^{(m)}}{1-(\bar{\beta}/\bar{\omega}'_m)^2} \tag{19}$$

where

$$\mathbf{C}^S = \mathbf{U}^T\cdot\mathbf{S}\cdot\mathbf{U}; \qquad \mathbf{r}^{(n)} = \tfrac{2}{3}\mathbf{U}^T\cdot\mathbf{D}^{(n)}\cdot\mathbf{U}; \qquad \mathbf{r}'^{(m)} = \tfrac{2}{3}\mathbf{U}^T\cdot\mathbf{D}'^{(m)}\cdot\mathbf{U};$$

$$\bar{\omega}_n = \frac{2}{\sqrt{3}}\frac{1}{\delta_n}; \qquad \bar{\omega}'_m = \frac{2}{\sqrt{3}}\frac{1}{\delta'_m} \tag{20}$$

The above formulas satisfy the general conditions of Reference 6 for poles and residues, namely, $\bar{\omega}_n \approx 0(n)$ and $r^{(n)} \to 0$ as $n \to \infty$ sufficiently fast for the sums in (19) to converge. If $\bar{k} < N$, the unwanted $N-\bar{k}$ ports

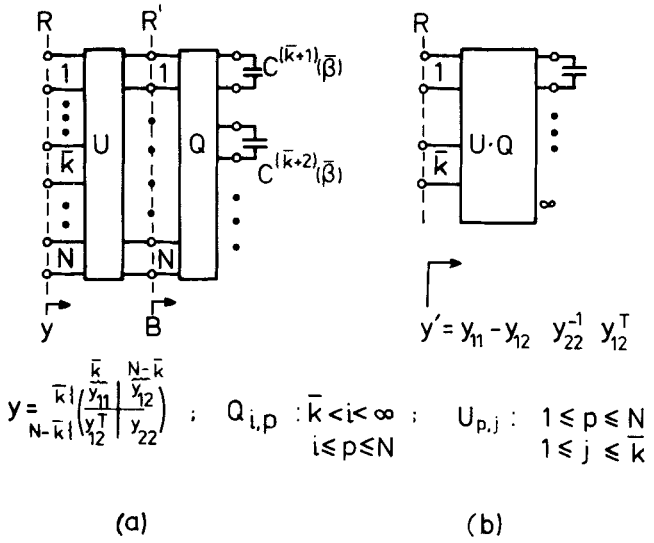

Figure 5. Ideal transformer embedding

are left open (see Figure 5(b)). The resulting equivalent network is then reduced to canonical form by means of standard transformations.

4. THICK IRIS

If the iris of Figure 1 has finite thickness, it can be treated as a cascade of two step discontinuities. In the important case of a thin iris in uniform waveguide ($t/d \ll 1$) the following is a more direct approach. The geometry of an iris of finite thickness 2t is illustrated in Figure 6(a). Thanks to its longitudinal symmetry, this structure can be analysed in terms of the even/odd excitation mode. A schematic equivalent circuit representation of the even/odd mode half structure is depicted in Figure 6(b). This consists of a lumped k_a-port, the first k ports corresponding to modes which are accessible in the guide. The remaining $k_a - k$ ports, i.e. the accessible modes in the iris are terminated by a magnetic/electric wall at reference plane T. Consistent with our previous normalization, the characteristic admittance of the fundamental mode in the

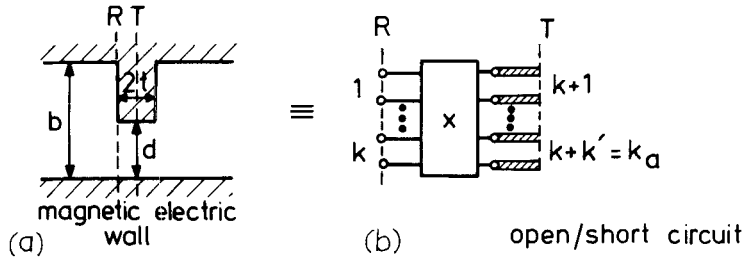

Figure 6. (a) Geometry thick iris, (b) even/odd mode equivalent network

iris is equal to unity. Furthermore, as mentioned in section 1, we have

$$x_{k+1,*} = x_{*,k+1} = \sqrt{\left(\frac{b}{d}\right)} x_{1*}$$

so that we need to consider only the reactance of a (k_a-1)-port ($\bar{k} = k_a - 1 = k+k'-1$). The waveguide susceptance matrix appropriate to the configuration of Figure 6 is obtained from (8) by setting $b' = d$ and replacing β/γ_m by

$$\beta/\gamma_m \begin{cases} \tanh \gamma_m t \\ \coth \gamma_m t \end{cases}$$

so that we have

$$\mathbf{B}_{pq} = \sum_{n \geq k} \frac{\beta}{\Gamma_n} P_{np} P_{nq} \varepsilon_{po} \varepsilon_{qo} + \sum_{m \geq k'} \frac{\beta}{\gamma_m} \frac{d}{b} A_{mp} A_{mq} \varepsilon_{po} \varepsilon_{qo} \begin{cases} \tanh \gamma_m t \\ \coth \gamma_m t \end{cases} \tag{21}$$

A convenient pr approximation of the driving point susceptance of the localized modes in the iris for $(\gamma_m - m\pi/d)t \ll 1 ; 1 \leqslant m \leqslant m_d$ is

$$\frac{\beta}{\gamma_m} \tanh \gamma_m t \simeq \frac{\beta}{\gamma_m} \frac{\tanh (m\pi t/d) + (\gamma_m - m\pi/d)t}{1 + \tanh (m\pi t/d) \cdot (\gamma_m - m\pi/d)t} \simeq \delta'_m \tanh \frac{m\pi t}{d} \cdot \frac{\bar{\beta}}{1 - \frac{1}{2}(\delta'_m \bar{\beta})^2}$$
$$\times \frac{1 - \frac{1}{2}(m\pi t/d) \cdot \coth (m\pi t/d)(\delta'_m \cdot \bar{\beta})^2}{1 - \frac{1}{2}(m\pi t/d) \cdot \tanh (m\pi t/d)(\delta'_m \cdot \bar{\beta})^2} \tag{22a}$$

for the even case, and for the odd case:

$$\frac{\beta}{\gamma_m} \coth \gamma_m t \simeq \delta'_m \cdot \coth \frac{m\pi t}{d} \cdot \frac{\bar{\beta}}{1 - \frac{1}{2}(\delta'_m \bar{\beta})^2} \cdot \frac{1 - \frac{1}{2}(m\pi t/d) \cdot \tanh (m\pi t/d) \cdot (\delta'_m \bar{\beta})^2}{1 - \frac{1}{2}(m\pi t/d) \cdot \coth (m\pi t/d) \cdot (\delta'_m \bar{\beta})^2} \tag{22b}$$

Usually, however, the quasi-static approximation:

$$\frac{\beta}{\gamma_m} \begin{cases} \tanh \gamma_m t \\ \coth \gamma_m \end{cases} \simeq \delta'_m \cdot \bar{\beta} \cdot \begin{cases} \tanh (m\pi t/d) \\ \coth (m\pi t/d) \end{cases} \tag{23}$$

strictly valid for $(\bar{\beta}\, \delta'_m)^2 \ll 1$, proves quite satisfactory. Introducing (22) or (23) in (21) and subsequently in (18), we obtain an expression for the susceptance $\mathbf{y}(\bar{\beta})$ of the accessible modes analogous to (19). Using (23), for instance, the quasi-static matrix $\mathbf{S}$, corresponding to S of (17a), is now:

$$\mathbf{S} = \eta - \sum_{n=1}^{n_d} D^{(n)} + \tfrac{1}{3} \sum_{n=k}^{n_d} D^{(n)} + \sum_{m>k'} D'^{(m)} \begin{cases} \tanh (m\pi t/d) \\ \coth (m\pi t/d) \end{cases} \tag{24}$$

The dynamic contribution is due to waveguide only and is identical to that of (16).

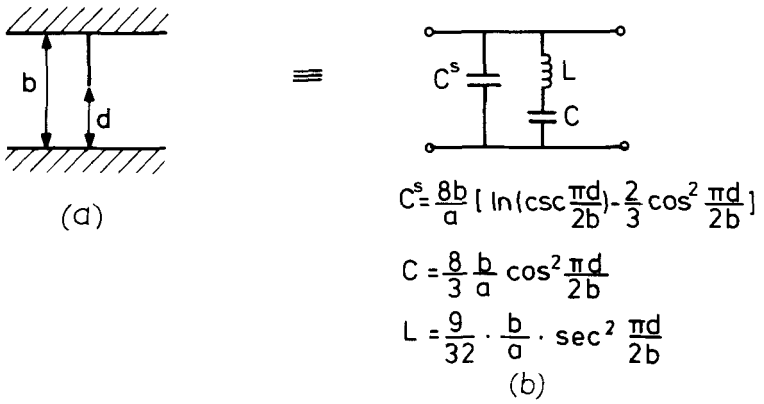

Figure 7. (a) Geometry infinitely thin iris, (b) approximate network representation ($N = k = n_d = 1$)

5. EXAMPLES AND DESIGN INFORMATION

(a) *Infinitely thin iris*

Setting $b = b'$ in Figure 2, one recovers the case of the infinitely thin iris in waveguide. If the guide is operating in its fundamental mode and in absence of interaction, that is, for one accessible mode, the equivalent circuit of the iris consists of a shunt susceptance across the transmission line representing the fundamental mode. A convenient approximation of the susceptance is obtained from (19) by setting $N = \bar{k} = 1$, corresponding to a first order variational solution for one accessible mode, and considering just one resonant term ($n_d = 1$). The resulting equivalent network is shown in Figure 7. In the case of two accessible modes, such as is the case in an oversize guide or in the case of interaction in a standard guide, the four-port equivalent circuit of Figure 8 is applicable.

This is obtained by setting $N = \bar{k} = n_d = 2$ in (19), corresponding to a second order variational solution for two accessible modes with two resonant terms. Of course, if the guide is standard, a representation of the isolated iris more accurate than that of Figure 7 is obtained either by closing ports 3 and 4 in Figure 8 by the characteristic admittance of the second mode, or by taking $N, n_d > 1$, $\bar{k} = 1$ in (19), leaving the unwanted $(N-1)$ ports open and simplifying the resulting network.

The accuracy of the above representations will now be tested by means of a numerical example. By setting $b/d = 1/2$ ($b = b'$) in Figure 2, one recovers the case of the infinitely thin semidiaphragm. For one accessible mode, this is the only case where an analytical solution to the iris problem exists. This result, given in Reference 2, p. 452 is obtained by integral transform techniques and involves the summation of a slowly convergent series. Also, $b/d = 1/2$ corresponds to maximum higher order mode excitation and is a 'worst case' for the approximate representations of Reference 1. Therefore it is interesting to check the previous theory against the exact solution in this case.

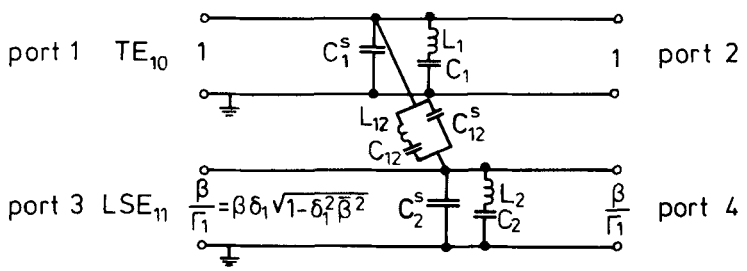

Figure 8. Infinitely thin iris; two accessible modes ($N = k = n_d = 2$)

Table I. Reflection coefficient of capacitive semidiaphragm: Figure 7(a) with $b/a = 4/9$; $d/b = 1/2$

$\bar{\omega}$	1 Exact	2 'Spot freq.' $N = 1$	3 'Spot freq.' $N = 2$	4 $N = n_d = k = 2$	5 $N = n_d = k = 1$
1·1	0·1420	0·1420	0·1420	0·1420	0·1419
1·2	0·2068	0·2069	0·2068	0·2068	0·2066
1·3	0·2609	0·2611	0·2609	0·2608	0·2606
1·4	0·3103	0·3107	0·3104	0·3101	0·3099
1·5	0·3574	0·3582	0·3574	0·3570	0·3569
1·6	0·4034	0·4050	0·4034	0·4029	0·4030
1·7	0·4492	0·4520	0·4493	0·4486	0·4492
1·8	0·4955	0·5001	0·4956	0·4947	0·4960
1·9	0·5431	0·5503	0·5431	0·5421	0·5442

A comparison over the 'fundamental mode' octave $1 < \bar{\omega} < 2$ for a standard aspect ratio $b/a = 4/9$ is shown in Table I. In column 1 is shown the reflection coefficient, computed according to Reference 2, after setting $\lambda \to \lambda_g$, as appropriate to a rectangular waveguide configuration. Column 2 displays the results of the 'spot-frequency' first order solution ($N = 1$ in (9)). As discussed in Reference 2, pp. 344–346, the variational solution gives here values in excess. Also, consistently with (16) and (21), the exact value is approached in the quasi-state limit $\bar{\omega}^2 \to 1$ ($\bar{\beta}^2 \to 0$), whereas the second order solution ($N = 2$), given in column 3, can be considered virtually 'exact' over the band. Column 4 was computed from the equivalent circuit of Figure 8, after closing ports 3 and 4 with the characteristic admittance of the second mode, here below cutoff. The maximum relative error is $\simeq 0{\cdot}18$ per cent and occurs at the upper band edge, as expected, since the frequency approximation deteriorates with increasing frequency. Finally, column 5 was computed from the equivalent circuit of Figure 7. Here the error is also $\approx 0{\cdot}18$ per cent owing to a compensation effect between the error (in excess) intrinsic in the variational solution and the error (in defect) arising from truncation of the expansion of the susceptance after the first resonant term.

(b) *E-plane step*

The waveguide step obtains by setting $b' = d$ in Figure 2(a). The resulting equivalent circuit for one accessible mode in the waveguide is shown in Figure 9.

The value of the shunt admittance to the left of the ideal transformer for $0{\cdot}1 \leqslant d/b \leqslant 0{\cdot}8$ and $\bar{\omega} = 1{\cdot}3454$ ($2b/\lambda_g = 0{\cdot}4$) is shown in Table II. The first column is obtained from the rather accurate formula 5·26a of Reference 1. In the second column, the first three values were computed from equation 5.26d of the same reference (small aperture approximation), the remaining two points from equation 5.26e (large aperture approximation). Column 3 shows the results computed according to the first order variational solution of Reference 10. Column 4 was computed with the present approach assuming $N = n_d = 2$, $m_d = 1$. Finally, column 5 was obtained from the simplified equivalent circuit of Figure 9 ($N = n_d = m_d = 1$). This corresponds to a first order variational solution, with one higher order mode only treated dynamically at each side of the step. The elements C and r', functions of the only geometric parameter d/b, can be derived from the plots in the figure. The remaining network elements are given by simple analytic expressions.

Table II(a). Normalized shunt susceptance of waveguide E-plane step (Figure 9) $b/a = 4/9$; $\bar{\omega} = 1{\cdot}3454$

d/b	1 Ref. 1, 5.263	2 Ibid. 5.26 d/e	3 Ref. 10 variat.	4 $N = 2$	5 $N = 1$
0·1	1·63	1·597	1·654	1·616	1·675
0·2	1·07	1·044	1·095	1·058	1·117
0·4	0·504	0·4985	0·5409	0·5082	0·5567
0·6	0·212	0·2091	0·2404	0·2184	0·2498
0·8		0·0554	0·0685	0·0606	0·0733

Table II(b). Modulus reflection coefficient of waveguide E-plane step

d/b	1	2	3	4	5
0·1	0·8225	0·8223	0·8226	0·8224	0·8227
0·2	0·6794	0·6788	0·6800	0·6791	0·6803
0·4	0·4475	0·4471	0·4502	0·4478	0·4515
0·6	0·2615	0·2612	0·2647	0·2622	0·2658
0·8		0·1138	0·1151	0·1143	0·1157

The values of the reflection modulus corresponding to the values given in Table II(a) are shown in Table II(b). These indicate that the above simple model is quite accurate for isolated steps up to relatively large values of d/b.

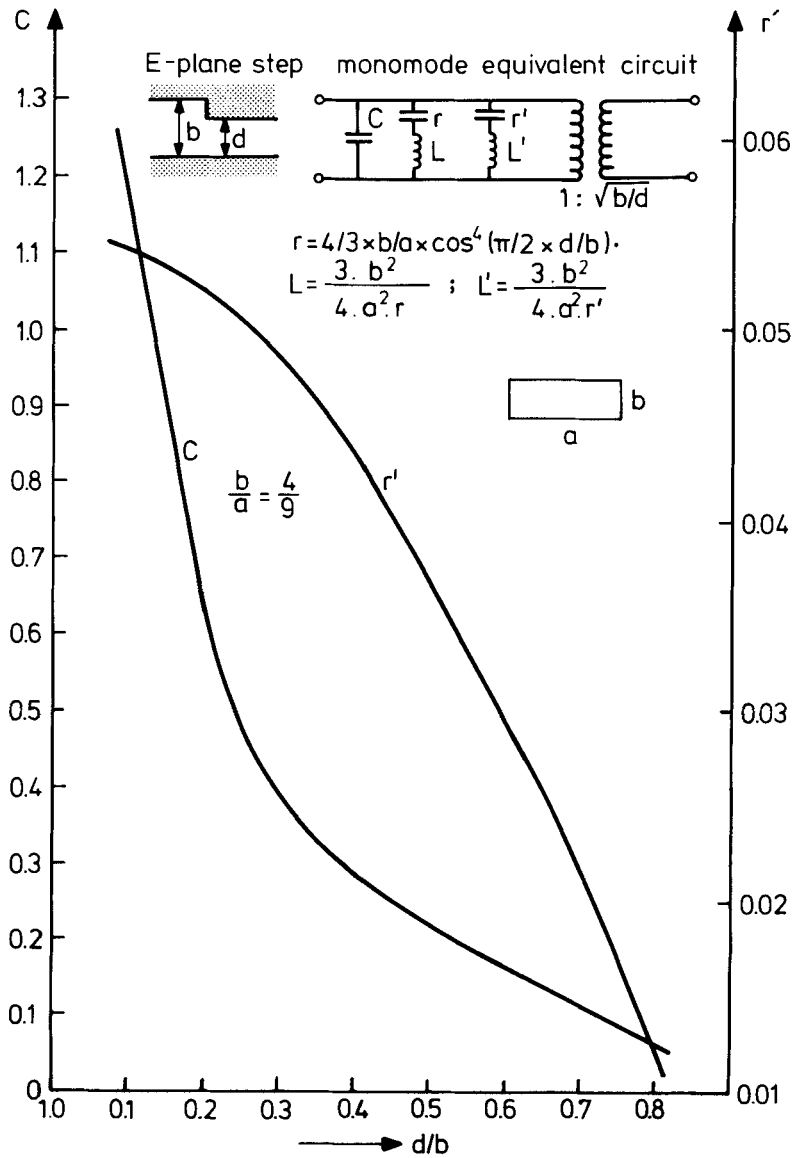

Figure 9. E-plane step: geometry and equivalent network

(c) *Thick iris*

A simple network model for a single thick iris is shown in Figure 10. The element values are plotted in Figures 11, 12. These were obtained with the approach of section 3 and setting $N = k = n_d = 1$, $m_d = 0$,

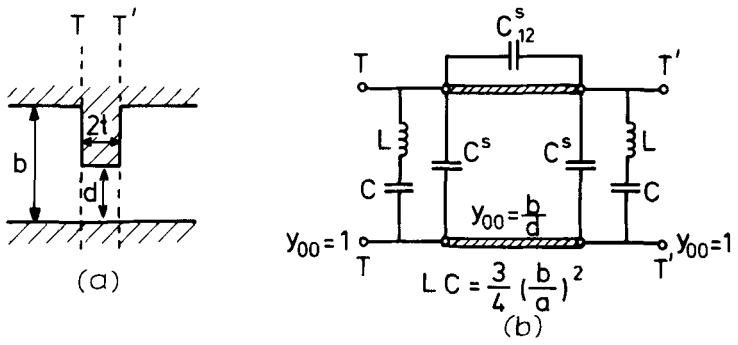

Figure 10. (a) Geometry thick iris, (b) approximate equivalent network ($N = k = n_d = 1$, $m_d = 0$)

i.e. assuming a first order variational solution, one accessible mode in the waveguide, treating dynamically, the first higher order mode in the guide and quasi-statically all higher order modes in the iris. Obviously, this model deteriorates for increasing $(d/a)\bar{\omega}$, while a simple double step model, neglecting interaction *via* higher order iris modes, becomes preferable in the case of very thick irises. Nevertheless the above model appears to be quite satisfactory in the frequency range $1 < \bar{\omega} < 2$, and within a wide range of thickness. Figure 13 shows computed values of the reflection modules vs. d/a at $\bar{\omega} = 1{\cdot}5$ for a very thin iris ($2t/a = 0{\cdot}001$) and a rather thick one ($2t/a = 0{\cdot}1$). For comparison, the results obtained with the small aperture/thick iris approach and the large aperture/thin iris approach of Reference 1 are also plotted. One notices that the results of the present method move gradually from those of the small aperture approach towards those of

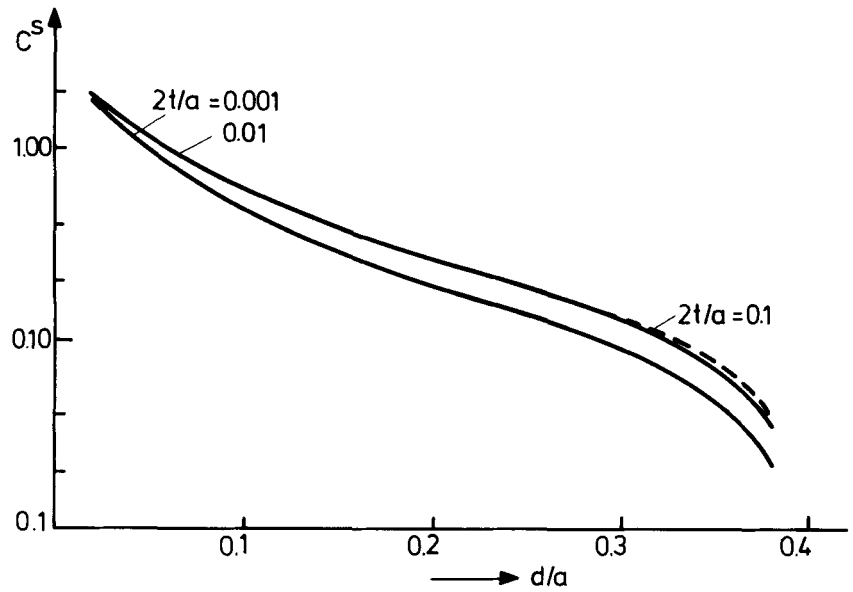

Figure 11. Normalized capacitance C^s of Figure 10 vs. d/a ($b/a = 4/9$)

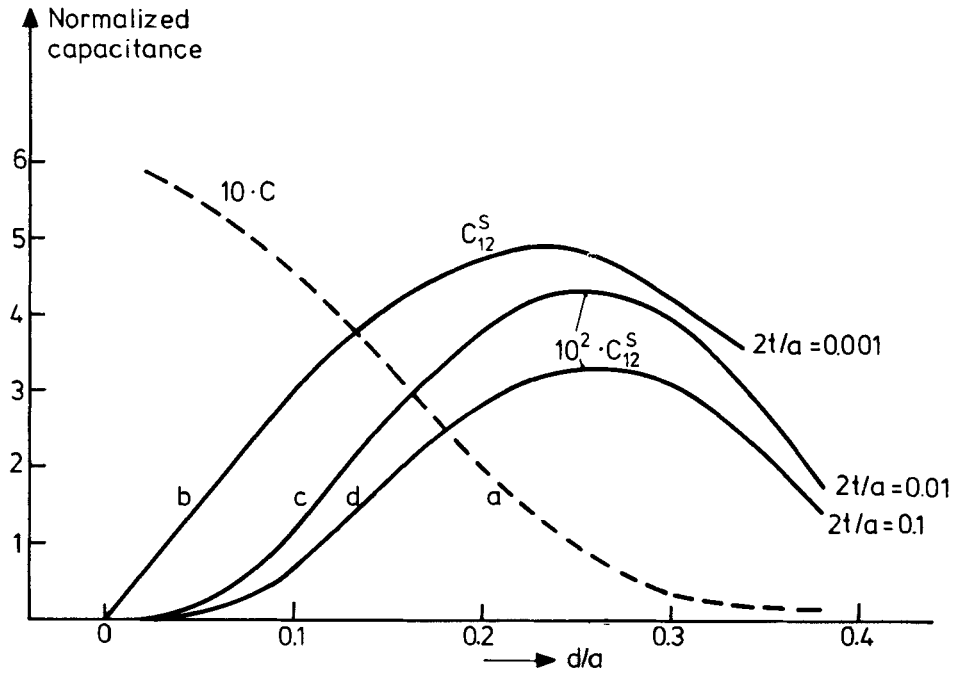

Figure 12. (a) Normalized C of Figure 10 vs. d/a (b/a = 4/9). (b), (c), (d). Normalized C_{12} of Figure 10 vs. d/a (b/a = 4/9) for $2t/a$ = 0·001, 0·01, 0·1 respectively

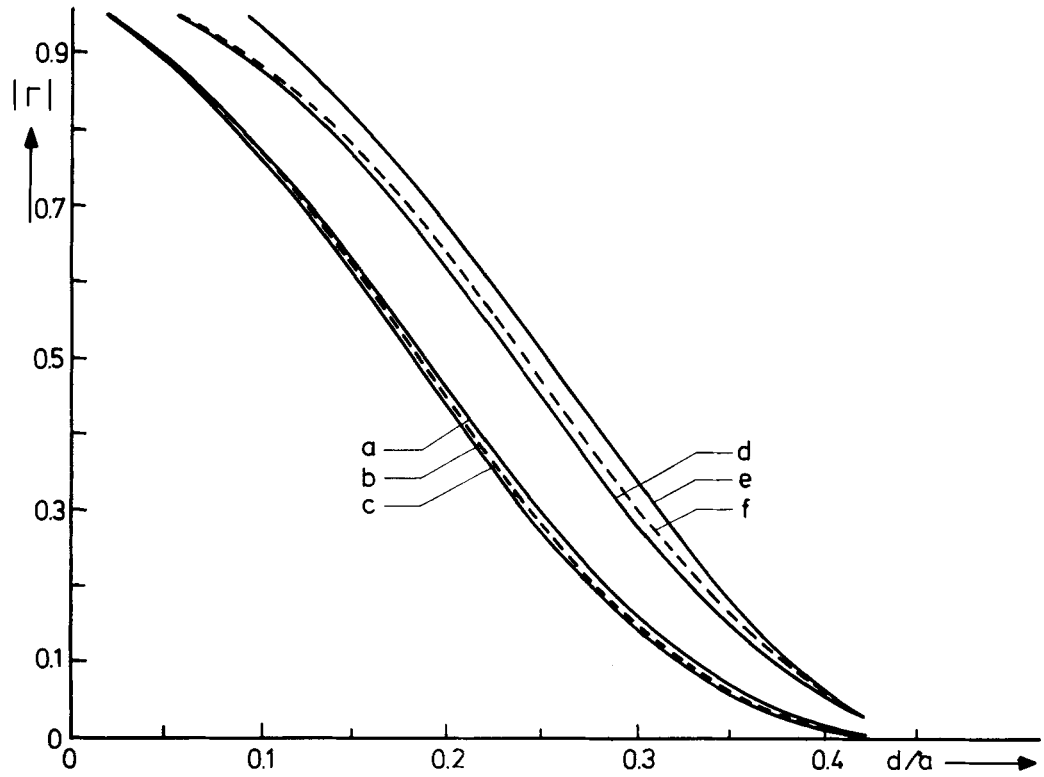

Figure 13. Computed modulus reflection coefficient thick iris vs. d/a for $\bar{\omega}$ = 1·5, b/a = 4/9. (a) Small aperture/thick iris Ref. 1, $2t/a$ = 0·001. (b) Large aperture/thin iris Ref. 1, $2t/a$ = 0·001. (c) Present theory, model of Figure 11(b), (d), (e), (f) Same as above for $2t/a$ = 0·1

Table III. Reflection coefficient thick iris (Figure 10(a))
a = 2·296 cm, b = 1·016 cm

Freq. = 9 GHz			
d	$\|\Gamma\|$ meas. (Ref. 11)	Computed $N = 1$ (Fig. 10(b))	$N = 2$
0·0254	0·9804	0·9809	0·9804
0·0381	0·9639	0·9699	0·9689
0·0508	0·9575	0·9590	0·9574
Freq. = 9·5 GHz			
	0·9845	0·9847	0·9843
	0·9729	0·9759	0·9751
	0·9662	0·9671	0·9658

the large aperture approach with increasing d/a. Also, the present curve lies closer to the relevant one of Reference 1 for both thicknesses. A comparison with experimental results for a thick iris of small aperture, taken from Reference 11, is shown in Table III.

(d) *Interaction via higher order modes*

If more than one mode is propagating in the guide or if two discontinuities are placed sufficiently close to each other, a two port representation no longer holds. According to the distance, additional modes, that is,

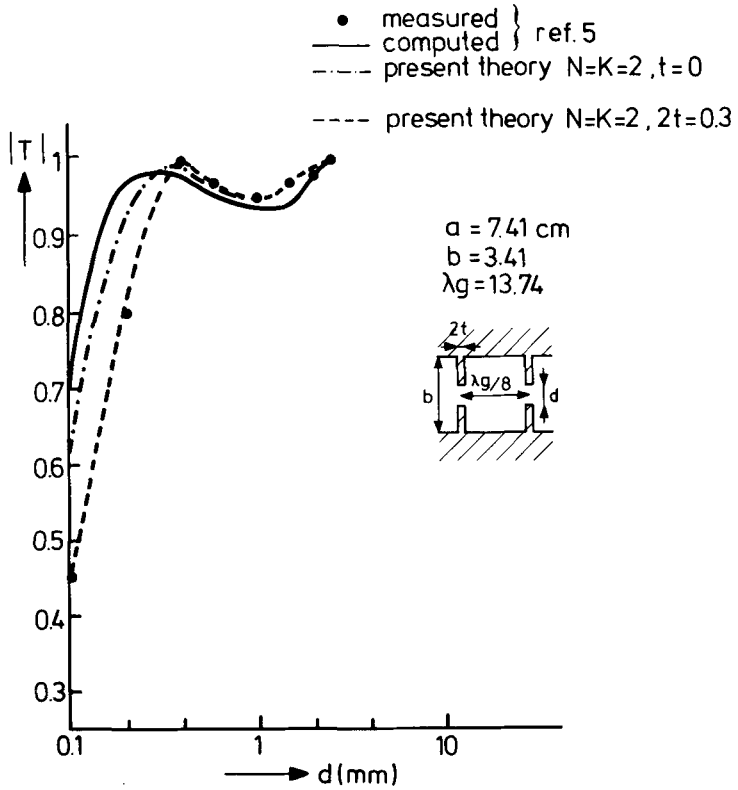

Figure 14. Modulus transmission coefficient of two identical interacting irises, spaced $\lambda_g/8$ apart vs. d. a = 7·41 cm; b = 3·41 cm; λ_g = 13·74 cm. (a) Computed, from Ref. 5, $t = 0$. (b) Present theory ($N = k = 2$), $t = 0$. (c) Present theory, $2t = 0{\cdot}3$ mm.

pairs of ports become accessible, so that the whole structure consists of a cascade of lumped multiports connected by parallel transmission lines, as shown in the schematic model of Figure 1(b). Because of interaction, the characteristics may differ considerably from those predicted by a two port model. This phenomenon has been studied by Bosma in the case of two infinitely thin identical symmetric irises in standard waveguide.[5]

Figure 14 compares computed (curve 1) and measured values of the transmission coefficient vs. iris aperture at one 'spot-frequency', as from the above reference, with those computed with the present approach. Curve 2 (present theory) was obtained by taking a second order variational solution ($N = 2$) for the infinitely thin iris and assuming two accessible modes in the region enclosed by the irises, which leads to the network model of Figure 8. Taking higher order variational solutions did not affect the results. Also, taking three accessible modes did not modify the characteristics appreciably, indicating that the interaction effect here is mainly due to the first higher order mode. The agreement between both computations and experiment can be considered very satisfactory, except for small values of d/b, where the actual thickness of the iris is no longer negligible. Introducing a small iris thickness (0·3 mm) in the computation improves the agreement in this region too, as shown by curve 3.

CONCLUSIONS

As shown by the examples of the previous section, it is possible to model capacitive irises and steps by means of simple and accurate equivalent networks. The network elements are found from field analysis. The design information provided should enable the designer to utilize the above results for synthesis.

ACKNOWLEDGEMENTS

The author is indebted to Mr. A. Skov, who carried out most of the numerical computations. It is a pleasant duty to thank Dr. W. F. G. Mecklenbräuker for various helpful discussions on the frequency approximations and for providing the subroutine for the computation of the coefficients of (7a), as well as Mr. F. C. de Ronde for his constructive criticism of the manuscript. Various discussions on computational aspects with Mr. J. F. Marchand, who provided the subroutine for the coefficients of (5), are also gratefully acknowledged.

APPENDIX

The susceptance matrix, realized by the equivalent network of Figure 8 follows from (19–20) setting $N = k = 2$. Of course, only the contribution from the larger waveguide must be considered in the above formulas and this must be multiplied by two, as discussed in (10).

From (19) one has

$$\mathbf{y}_{12} = \bar{\beta}\mathbf{C}^S_{12} + \frac{\bar{\beta}\mathbf{r}^{(2)}_{12}}{1-3(b/2a)^2\bar{\beta}^2} \tag{A.1}$$

so that

$$\bar{\mathbf{C}}^S_{12} = -\mathbf{C}^S_{12}; \qquad \mathbf{C}_{12} = -\mathbf{r}^{(2)}_{12};$$

Also

$$\mathbf{y}_{11}+\mathbf{y}_{12} = \bar{\beta}(\mathbf{C}^S_{11}+\mathbf{C}^S_{12}) + \frac{\bar{\beta}(\mathbf{r}^{(2)}_{11}+\mathbf{r}^{(2)}_{12})}{1-3(b/2a)^2\bar{\beta}^2} \tag{A.2}$$

$$\equiv \bar{\beta}\mathbf{C}^S_1 + \frac{\bar{\beta}C_1}{1-L_1C_1\bar{\beta}^2}$$

and similarly for $\mathbf{y}_{22}+\mathbf{y}_{12}$.

The matrices $\mathbf{r}^{(2)}$ and $\mathbf{C}^S$ are obtained from (20) by straightforward multiplication. Set:

$$\alpha_1 \equiv \cos^2 \frac{\pi d}{2b}; \qquad \alpha_2 = 1-\alpha_1; \qquad s = \ln\left(\csc\left(\frac{\pi d}{2b}\right)\right)$$

$$A = 1-\tfrac{8}{3}\alpha_1+4\alpha_1^2; \qquad B = 1/\alpha_2^2-(1+\tfrac{16}{3}\alpha_1^2); \qquad D = \tfrac{1}{3}+\tfrac{4}{3}\alpha_1-5\alpha_1^2$$

One has then:

$$\mathbf{r}^{(2)} = \frac{2b}{3a}\begin{pmatrix} 2\alpha_1^2(\alpha_1+2)^2 & -4\sqrt{(2)}\alpha_1^2(2+\alpha_1) \\ -4\sqrt{(2)}\alpha_1^2(2+\alpha_1) & 16\alpha_1^2 \end{pmatrix} \tag{A.3}$$

$$\mathbf{C}^S = \frac{2b}{a}\begin{pmatrix} 2[s+\alpha_1^2(B-D)] & -\sqrt{2}\,\alpha_1(A+B) \\ -\sqrt{2}\,\alpha_1(A+B) & B \end{pmatrix} \tag{A.4}$$

The above are positive semidefinite matrices, as it should be. due to the pr character of the frequency approximation. In particular $\mathbf{r}^{(2)}$ is the residue matrix of a compact network. In the network representation of Figure 8, the element values are:

$$\bar{C}_{12}^s = \frac{2b}{a}\sqrt{2}\,\alpha_1(A+B)$$

$$C_1^s = \frac{2b}{a}[2s+2\alpha_1^2(B-D)-\sqrt{2}\,\alpha_1(A+B)]$$

$$C_2^s = \frac{2b}{a}[B-\sqrt{2}\,\alpha_1(A+B)]$$

$$C_1 = \frac{4b}{3a}\alpha_1^2(\alpha_1+2)[\alpha_1+2(1-\sqrt{2})]; \qquad L_1 = 3\left(\frac{b}{2a}\right)^2/C_1$$

$$C_{12} = \frac{8b}{3a}\sqrt{2}\,\alpha_1^2(\alpha_1+2); \qquad L_{12} = 3\left(\frac{b}{2a}\right)^2/C_{12}$$

$$C_2 = \frac{8b}{3a}2\alpha_1^2[2(\sqrt{2}-1)-\alpha_1]; \qquad L_2 = 3\left(\frac{b}{2a}\right)^2/C_2$$

Compatibly with positive reality, some of the elements above may become negative, indicating the presence of an ideal transformer.

REFERENCES

1. N. Marcuvitz, *Waveguide Handbook*, chs 5, 8, McGraw-Hill, New York, 1951.
2. R. Collin, *Field Theory of Guided Waves*, ch 8, McGraw-Hill, New York, 1960.
3. J. Schwinger and D. Saxon, *Discontinuities in Waveguides*, ch 5, Gordon and Breach, London, 1968.
4. R. Mittra, T. Itoh and T. S. Li, 'Analytical and numerical studies of the relative convergence phenomenon arising in the solution of an integral equation by the moment method', *IEEE Trans. Microwave Theory Techn.* MTT-**20**, 96–104 (1972).
5. H. Bosma, 'Two capacitive windows in a rectangular waveguide', *Appl. Sci. Res.*, B **7**, 131–144 (1959).
6. T. E. Rozzi, 'Network analysis of strongly coupled transverse apertures in waveguide', *Int. J. Cir. Theor. Appl.* **1**, 161–178 (1973).
7. T. E. Rozzi and W. Mecklenbräuker, 'Field and network analysis of waveguide discontinuities', *Proc. 1973 European Microwave Conf.*, paper B.1.2, Brussels, 1973.
8. T. E. Rozzi and W. Mecklenbräuker, 'Wideband network modelling of interacting inductive irises and steps', *IEEE Trans. Microwave Theory Techn.* MTT **23**, 235–245 (1975).
9. O. Perron, *Die Lehre von Kettenbrüchen*', p. 320, Chelsea, New York.
10. L. Lewin, *Advanced Theory of Waveguides*, Chap. 5, Iliffe, London, 1951.
11. M. Potok, 'Capacitive-iris-type mechanically tunable waveguide filters for X-band', *Proc. IEE*, B **48**, 505–510 (1962).